Available online at www.sciencedirect.com

SCIENCE DIRECT®

Surface Science 524 (2003) 173–182

SURFACE SCIENCE

www.elsevier.com/locate/susc

An infrared spectroscopic and temperature-programmed desorption study of methyl iodide hydrogenation on Pd(1 1 1)

D. Stacchiola, Y. Wang, W.T. Tysoe *

Department of Chemistry and Laboratory for Surface Studies, University of Wisconsin-Milwaukee, P.O. Box 413, Milwaukee, WI 53211, USA

Received 26 August 2002; accepted for publication 30 October 2002

Abstract

The adsorption and hydrogenation of methyl iodide is studied on clean and hydrogen-covered Pd(1 1 1) using reflection–adsorption infrared spectroscopy (RAIRS) and temperature-programmed desorption. Molecular methyl iodide desorbs from clean Pd(1 1 1) at 229 K and hydrogen desorbs at ~360 K. Methyl groups hydrogenate in two states at 191 and 304 K for large methyl iodide exposures where RAIRS data suggest that the low-temperature state is due to reaction with tilted methyl species while the high-temperature state is formed by hydrogenation of perpendicular ones. A single state is found at low methyl iodide coverages at ~219 K due to the hydrogenation of tilted methyl species where the kinetics is limited by the rate of α-hydrogen elimination. Saturating the surface with hydrogen completely suppresses the high-temperature methane desorption state and the methane desorbs at between 189 and 207 K depending on coverage.

Keywords: Palladium; Halides; Infrared absorption spectroscopy; Thermal desorption spectroscopy; Surface chemical reaction

1. Introduction

Iodine-containing molecules have been extensively used to deposit hydrocarbon fragments onto transition-metal surfaces to provide a fundamental understanding of catalytic hydrocarbon conversion reactions, such as Fisher–Tropsch synthesis, olefin metathesis and alkene hydrogenation [1–3]. It was previously shown that ethyl species formed on Pd(1 1 1) from ethyl iodide reacted with hydrogen to form ethane much more rapidly than did adsorbed ethylene, suggesting that the rate-limiting step in the reaction of adsorbed ethylene to ethane was the addition of the first hydrogen to ethylene to form an ethyl species [4]. In order to further understand these elementary hydrogenation steps on Pd(1 1 1), the surface chemistry and hydrogenation reactions of methyl species adsorbed on Pd(1 1 1) from its corresponding iodide is investigated in the following. Methyl iodide adsorption and the formation of the corresponding methyl species have been previously studied on several transition metals [1,2]. Silver [5] and gold [6] appear to exhibit unique behaviors since alkyl

---

* Corresponding author. Tel.: +1-414-229-5222; fax: +1-414-229-5036.

E-mail address: wtt@uwm.edu (W.T. Tysoe).

0039-6028/02/$ - see front matter © 2002 Elsevier Science B.V. All rights reserved.
PII: S0039-6028(02)02529-3

species do not self-hydrogenate to methane on these surfaces, but rather tend to dimerize [7,8]. Methane formation is found due to the reductive elimination of methyl species on other transition metals surfaces at 215 K on Pd(1 0 0) [9], 230 K on Ni(1 0 0) [10] and 260 K on Pt(1 1 1) [11]. Previous temperature-programmed desorption (TPD) studies of CH_3I and CD_3I on Pd(1 1 1) found only methane desorption at ~210 K due to reaction of methyl species with hydrogen contamination present in the bulk of the sample [12]. Hydrogen background contamination of palladium has been shown to be a problem even under ultrahigh vacuum conditions. Recent experiments, in which great care was taken to completely remove all hydrogen from the sample, have revealed differences with earlier work, even on extensively studied systems such as ethylene on Pd(1 1 1) [13].

The X-ray photoelectron spectra (XPS) of methyl iodide on Pd(1 1 1) have been collected previously [12,14] and reveal that substantial C–I bond cleavage is underway by 110 K and is essentially complete by 150 K. Similar conclusions were arrived at on Pd(1 0 0) [9], where XPS similarly indicated that C–I bond cleavage occurs between 150 and 170 K, so at slightly higher temperatures than on Pd(1 1 1).

Studies have been carried out on the reaction of methylene species, generated from CH_2I_2, with adsorbed oxygen [15–18], and methyl species [19]. In the case of palladium, XPS shows the thermal formation of methylene species from methylene iodide by ~200 K on Pd(1 0 0) [20] and ~130 K on Pd(1 1 0) [21].

It is shown in the following that adsorbed methyl species on Pd(1 1 1) hydrogenate in two states at 191 and 304 K where the low-temperature state is due to reaction with tilted methyl species while the high-temperature state is due to reaction with perpendicular ones. Addition of hydrogen to Pd(1 1 1) forms methane at between 189 and 207 K depending on coverage.

2. Experimental

Experiments were carried out in two stainless-steel, ultrahigh vacuum chambers operating at base pressures of $\sim 8 \times 10^{-11}$ Torr following bakeout, and which have been described in detail elsewhere [22,23]. Infrared data were collected from a Pd(1 1 1) single crystal sample mounted in a modified 2 3/4" six-way cross equipped with infrared-transparent, KBr windows. The sample could be resistively heated to 1000 K, or cooled to 80 K using liquid nitrogen. Light from a Bruker Equinox infrared spectrometer passed through a polarizer and was focused onto the sample at an incidence angle of ~80°, and the reflected light steered onto the detector of a liquid-nitrogen-cooled, mercury cadmium telluride detector. The complete light path was enclosed and purged with dry, CO_2-free air. The spectrometer operated at 4-cm^{-1} resolution and data were typically collected for 1000 scans.

TPD spectra were collected in a separate ultrahigh vacuum chamber [23] where the sample could be similarly heated and cooled and could be placed in front of a Dycor quadrupole mass analyzer to collect TPD data.

In both cases, the sample was cleaned using a standard procedure and the absence of carbon, the main contaminant after annealing the sample, was confirmed by the absence of CO detected in TPD after dosing the surface with oxygen.

The methyl iodide (Aldrich Chemicals, 99%), methylene iodide (Aldrich Chemicals, 99.9%), ethyl iodide (Aldrich Chemicals, 99%) and perdeuterated CD_3I (Aldrich Chemicals, 99%D) were transferred to glass vials, attached to the gas-handling line of the vacuum system, and further purified by repeated freeze–pump–thaw cycles and their purities monitored mass spectroscopically.

3. Results

3.1. Methyl iodide adsorption on Pd(111)

Fig. 1 shows a series of TPD spectra, collected using a heating rate of 7 K/s, of 6 L ($1\ L = 1 \times 10^{-6}$ Torr s) of CD_3I adsorbed on Pd(1 1 1) at 80 K. Exposures are not corrected for ionization gauge sensitivities and this exposure produces slightly more than the saturation coverage. The 145-amu spectrum is due to the desorption of molecular

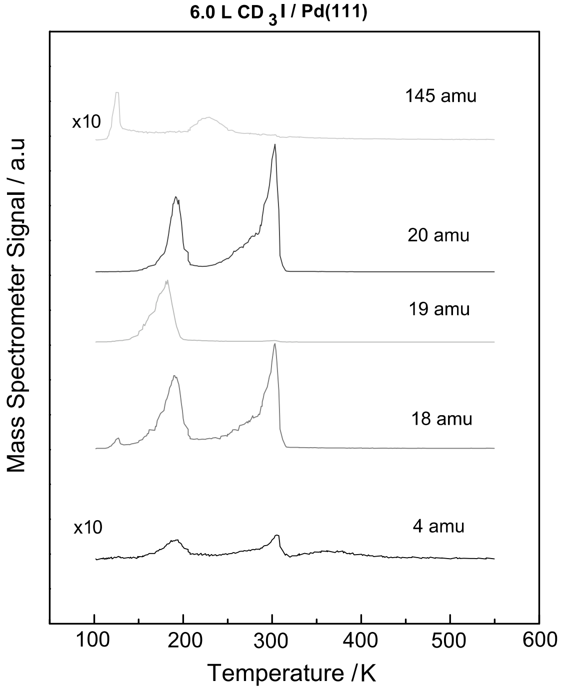

Fig. 1. Survey TPD spectra of CD_3I (6 L) adsorbed on Pd(1 1 1) at 80 K collected using a heating rate of 7 K/s monitoring 4 (D_2), 18 (CD_3), 19 (CD_3H), 20 (CD_4) and 145 (CD_3I) amu. The monitored masses are marked adjacent to the corresponding spectrum.

methyl iodide and exhibits a sharp peak at 127 K which also has a fragment at 18 amu. This feature continues to grow with increasing exposure and is assigned to the desorption of methyl iodide multilayers. An additional molecular desorption feature is detected at 229 K where the corresponding 18-amu fragment is obscured by the large features at 191 and 304 K in the 18-amu spectrum. This desorption temperature is between that found from Pt(1 1 1) of ~235 K [11] and that from Ag(1 1 1) of ~211 K [5]. Intense features are detected at 191 and 304 K in the 20- and 18-amu spectra and are assigned to the desorption of methane (CD_4). Features are evident at these temperatures at 4 amu indicating that these are due to fragmentation of the desorbing methane in the mass spectrometer ionizer. A small feature is detected in the 4-amu spectrum at ~360 K due to the desorption of molecular D_2 and the weakness of this signal indicates that the majority of the surface hydrogen reacts rapidly with adsorbed methyl species to form methane. A feature is detected for the 19-amu fragment at 179 K and is not due to fragmentation of desorbing CD_4 in the mass spectrometer ionizer and is possibly due to the formation of some CD_3H by reaction between adsorbed CD_3 species and residual hydrogen in the sample.

Fig. 2 shows the evolution of the 20-amu (methane) desorption state as a function of CD_3I exposure, where the exposures are marked adjacent to the corresponding spectrum. This displays a relatively complex behavior having a single methane desorption state at 219 K for exposures up to 2.0 L, which splits into two states as the exposure exceeds 3.0 L, eventually forming two desorption states at 191 and 304 K after a 6-L exposure, as shown in Fig. 1.

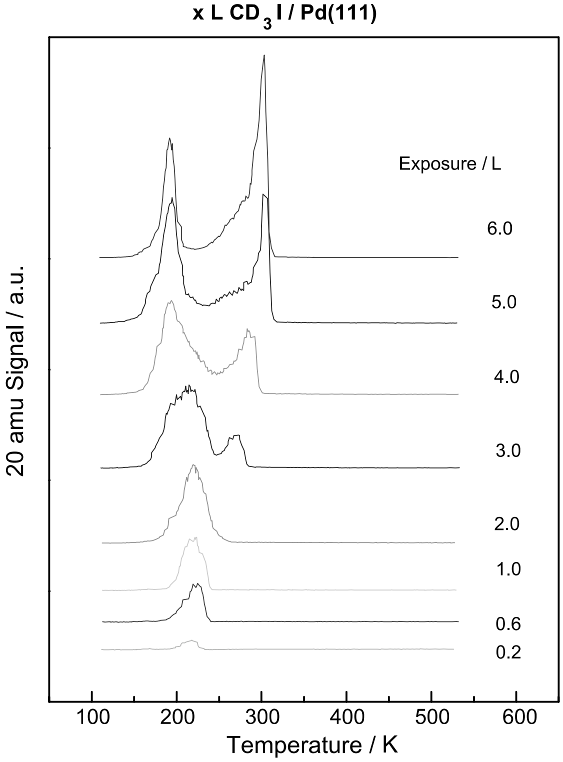

Fig. 2. TPD spectra of CD_3I adsorbed on Pd(1 1 1) at 80 K collected using a heating rate of 7 K/s monitoring 20 amu (CD_3) as a function of CD_3I exposures, where the exposures (in Langmuirs) are marked adjacent to the corresponding spectrum.

The corresponding 4-amu (D_2) spectra are displayed in Fig. 3. These show the 219-, 191- and 304-K peaks due to fragments of the CD_4 desorption state evident in Fig. 2. An additional feature is seen at ~359 K due to the desorption of residual deuterium from the Pd(1 1 1) surface and the intensity of this feature remains relatively constant up to an exposure of 1 L. It decrease in intensity at exposures above 2 L, coincident with the onset of high-temperature CD_4 formation.

The effect of pre-dosing the surface with deuterium is shown in Figs. 4 and 5. Survey spectra are displayed in Fig. 4, collected after pre-dosing the Pd(1 1 1) surface with 10 L of D_2 and then exposing to 6 L of CD_3I. This exhibits a sharp multilayer desorption feature at 152 K (with fragments at 145, 18 and 4 amu). This temperature is slightly higher than the multilayer desorption state from clean Pd(1 1 1) (127 K, Fig. 1). Methane now desorbs in a single state centered at 209 K with mass spectrometer ionizer intensity at 20, 18 and 4 amu with a small amount of intensity at 19 amu. This is in good agreement with the desorption temperature of CD_3H from hydrogen-contaminated Pd(1 1 1) [12]. The 19-amu signal is also centered at 209 K indicating that this feature is not due to the interaction of adsorbed CD_3 species with residual hydrogen in the sample. Remaining deuterium desorbs from the surface at ~300 K. The evolution of the 20- and 18-amu (CD_4) TPD spectra with exposure is displayed in Fig. 5. These spectra exactly mirror each other confirming that they are due to CD_4 desorption from the surface. At low d_3-methyl iodide exposures (1 and 3 L), methane desorbs in a single feature centered at ~189 K. As the d_3-methyl iodide exposure increases, the methane desorption feature shifts to higher temperatures, but maintains a relatively

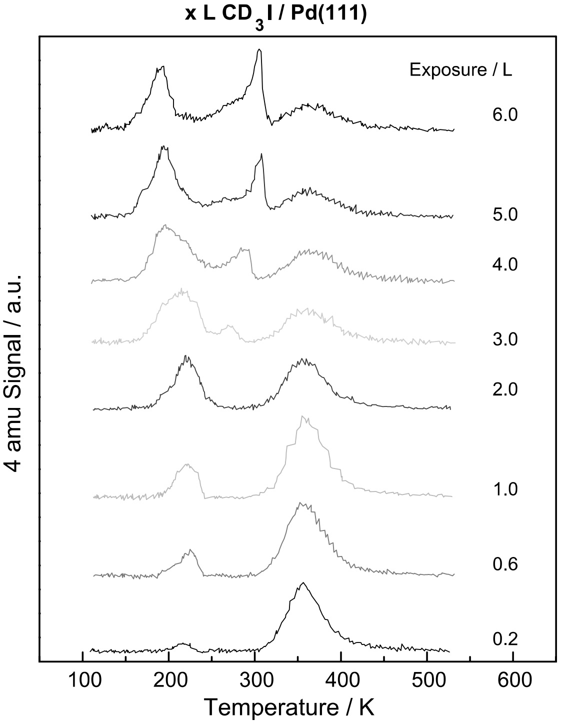

Fig. 3. TPD spectra of CD_3I adsorbed on Pd(1 1 1) at 80 K collected using a heating rate of 7 K/s monitoring 4 amu (D_2) as a function of CD_3I exposures, where the exposures (in Langmuirs) are marked adjacent to the corresponding spectrum.

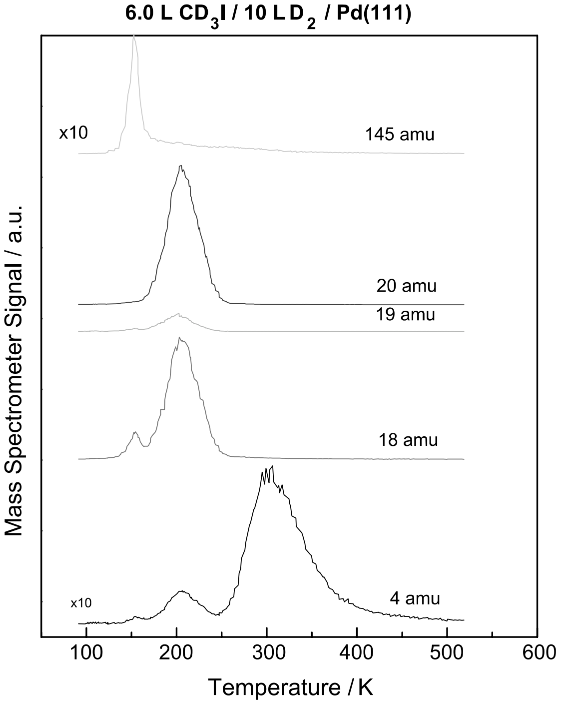

Fig. 4. Survey TPD spectra of CD_3I (6 L) adsorbed on deuterium-covered Pd(1 1 1) (following a 10-L D_2 exposure) at 80 K collected using a heating rate of 7 K/s monitoring 4 (D_2), 18 (CD_3), 19 (CD_3H), 20 (CD_4) and 145 (CD_3I) amu. The monitored masses are marked adjacent to the corresponding spectrum.

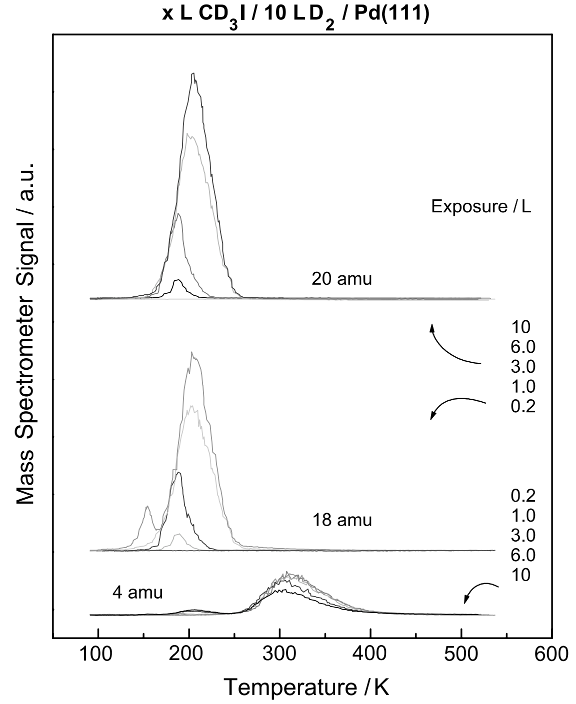

Fig. 5. TPD spectra of CD_3I adsorbed on deuterium-covered Pd(1 1 1) (following a 10-L deuterium exposure) collected using a heating rate of 7 K/s as a function of CD_3I exposure monitoring 4 (D_2), 18 (CD_3) and 20 (CD_4) amu. Both the masses and CD_3I exposures are marked adjacent to the corresponding spectra.

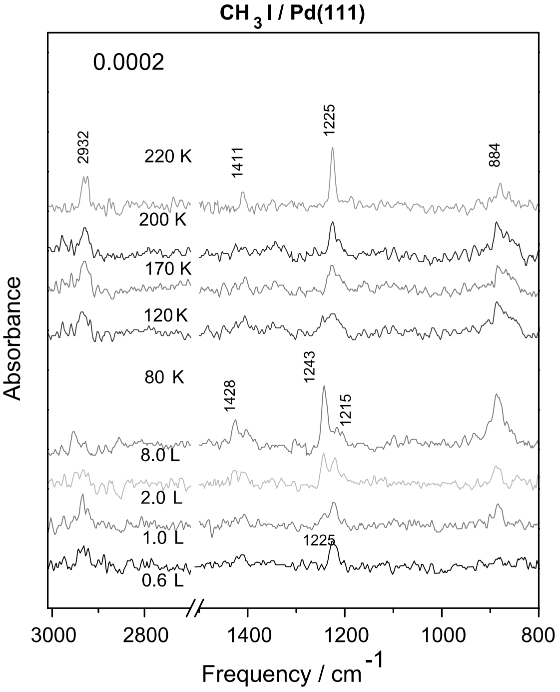

Fig. 6. Reflection infrared absorption spectrum of methyl iodide (CH_3I) adsorbed onto Pd(1 1 1) at 80 K as a function of methyl iodide exposure where these are marked adjacent to the corresponding spectrum. Also shown are spectra collected after heating to various temperatures where the annealing temperature are marked adjacent to the corresponding spectra.

common leading edge, so that after a CD_3I exposure of 10 L the methane desorption peak temperature has increased to 207 K.

The corresponding reflection–absorption infrared spectra (RAIRS) of CH_3I on Pd(1 1 1) are displayed in Fig. 6. The spectra of CD_3I were also collected (not shown) and exhibit features identical to those found on Pt(1 1 1) [11]. The bottom spectra in Fig. 6 are for increasing methyl iodide exposures at a sample temperature of 80 K (where the exposures are marked adjacent to the corresponding spectrum). These display features at 884, 1215, 1225, 1243, 1428 and 2932 cm^{-1}. The peaks at 1215 and 1411 cm^{-1} grow only slowly as a function of increasing methyl iodide exposure while those at 884, 1243 and 1428 cm^{-1} grow more rapidly without saturation. As the surface is heated to 120 K, the 1243- and 1428-cm^{-1} peaks essentially disappear while that at 884 cm^{-1} is substantially diminished in intensity. A broad feature is observed centered at 1225 cm^{-1}, which has been assigned to a compressed methyl iodide layer [11]. A temperature of 120 K corresponds to the multilayer desorption temperature in TPD (Fig. 1) and also that at which C–I bond cleavage takes place (between 110 and 150 K [12,14]). Thus, these features may either be assigned to compressed methyl iodide species on the Pd(1 1 1) surface [11] or to adsorbed methyl species and, most likely, to a combination of both. Note that molecular methyl iodide desorbs at $\sim$229 K (Fig. 1), so that the shoulder on the 1225-cm^{-1} feature after annealing to 200 K is likely due to remaining molecular species. Assignments are summarized in Table 1. The spectrum formed by heating to 170 K (when all of the multilayer has desorbed (Fig. 1), and C–I bond cleavage is complete [12,14]) shows the

Table 1
Assignments of the features in the RAIRS spectrum of 8 L of methyl iodide (C_{3v} symmetry) adsorbed on Pd(1 1 1) at 80 K (Fig. 6)

Symmetry	Mode	Gas-phase CH_3I/cm^{-1} [24]	CH_3I/Pd(1 1 1)/cm^{-1}
$e(x,y)$	$\nu_a(CH_3)$	3060	–
$a_1(z)$	$\nu_s(CH_3)$	2933	2932
$e(x,y)$	$\delta_a(CH_3)$	1436	1428
$a_1(z)$	$\delta_s(CH_3)$	1252	1215
$e(x,y)$	$\rho(CH_3)$	882	884

δ—deformation, ρ—rock, ν—stretch.

appearance of an additional sharper feature at 1225 cm^{-1}. As the surface is heated, the broad 1215-cm^{-1} mode loses some of its intensity and the 1225-cm^{-1} peak becomes sharper. After heating to 220 K, the spectrum consists of two sharp features at 1225 and 2932 cm^{-1}. This temperature corresponds to the completion of the low-temperature methane desorption state (Fig. 1), and the desorption of the residual molecular CH_3I. This suggests that a portion of the methyl species present on the surface at 120 K hydrogenates to methane yielding the 191-K methane desorption state and the species present at 220 K yields the high-temperature (304-K) state.

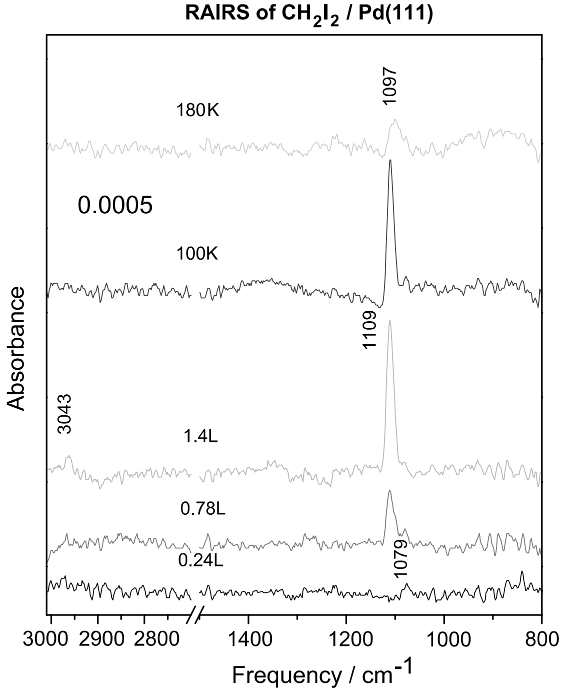

Fig. 7. Reflection infrared absorption spectrum of methylene iodide (CH_2I_2) adsorbed onto Pd(1 1 1) at 80 K as a function of methyl iodide exposure where these are marked adjacent to the corresponding spectrum. Also shown are spectra collected after heating to various temperatures where the annealing temperature are marked adjacent to the corresponding spectra.

Table 2
Assignments of the features in the RAIRS spectrum of methylene iodide (C_{2v} symmetry) adsorbed on Pd(1 1 1) at 80 K (Fig. 7)

Symmetry	Mode	Gas-phase frequency/cm^{-1} [24]	Frequency/cm^{-1}
$b_2(x)$	$\nu_a(CH_2)$	3047	3043
$a_1(z)$	$\nu_s(CH_2)$	2968	2960
$a_1(z)$	$\delta(CH_2)$	1349	–
$b_1(y)$	$\omega(CH_2)$	1103	1109
$a_2(–)$	$\gamma(CH_2)$	1028	–
$b_2(x)$	$\rho(CH_2)$	714	–

δ—deformation, ρ—rock, ν—stretch, γ—twist, ω—wag.

The reflection–absorption infrared spectra of CH_2I_2 adsorbed on Pd(1 1 1) are displayed in Fig. 7 both as a function of exposure (Fig. 7, bottom three spectra) and after heating the surface to various temperatures (Fig. 7, top two spectra). The exposures and annealing temperatures are displayed adjacent to the corresponding spectra. The spectra following adsorption at 80 K exhibit major features at 1109 and 3043 cm^{-1} which grow with increasing exposure, as well as a feature at 1079 cm^{-1} which is present at low exposures, but which does not grow as the exposure increases. The peaks that grow with exposure are due to molecular methylene iodide and can be assigned by comparison with the gas-phase spectrum and the assignments are displayed in Table 2. Two different arrangements of condensed layers have been identified when CH_2I_2 was deposited onto Al(1 1 1) [25] with features at 1109 and 1095 cm^{-1} and with a transition temperature between the two of ~130 K. Evidently modes of a_1, b_1 and b_2 symmetry are all detected on Pd(1 1 1) implying that the molecular overlayer adopts no preferential high-symmetry geometry on this surface. As the sample is heated to 100 K, the C–H stretching mode disappears leaving an intense feature at 1109 cm^{-1} (due to the $\omega(CH_2)$ mode). As the sample is heated to ~180 K, the 1109-cm^{-1} feature attenuates substantially in intensity, the peak at 1079 cm^{-1} persists, and a feature grows at ~1097 cm^{-1}. Features detected at 1061 cm^{-1} on Mo(1 0 0) [26] and 1097 cm^{-1} on Ag(1 1 1) [27] have been assigned to the presence of $CH_{2(ads)}$ and since a feature is present at close to this value at low coverages (1079 cm^{-1}, Fig. 7), it is likely that this feature is due to a similar species. These observations are in accord with those found for methylene iodide on Pd(1 0 0) [9] where some C–I bond cleavage was detected even at 90 K and where total dissociation occurred at between 160 and 230 K. If the principle C_2 axis of the methylene species were oriented perpendicular to the surface, only modes of a_1 symmetry should be allowed. However, the $\omega(CH_2)$ mode has b_1 symmetry (Table 2) which may indicate that this species is somewhat tilted with respect to the Pd(1 1 1) surface.

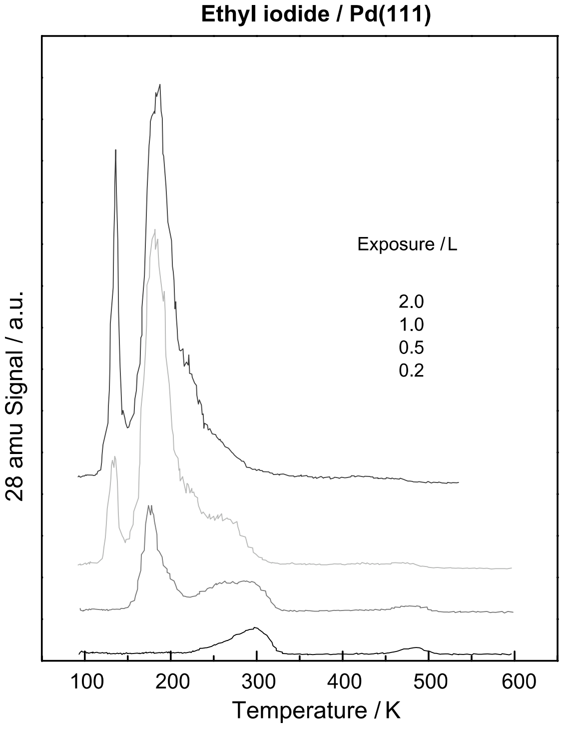

Fig. 8. TPD spectra of C_2H_5I adsorbed on Pd(1 1 1) at 80 K collected using a heating rate of 7 K/s as a function of C_2H_5I exposure monitoring 28 amu (ethylene). C_2H_5I exposures are marked adjacent to the corresponding spectra.

In order to compare the rates of α- and β-hydrogen elimination on Pd(1 1 1), a series of 28-amu TPD spectra were collected for ethyl iodide adsorbed on Pd(1 1 1) and the results are displayed in Fig. 8. These spectra were collected using exactly identical conditions to those for methyl iodide allowing direct comparison between the results. At low ethyl iodide exposures (0.2 L, Fig. 8), a small 28-amu feature is detected at 300 K. An additional feature appears at ~175 K for ethyl iodide exposures greater than 0.5 L and sharp feature is found at ~130 K at higher exposures assigned to the fragmentation of desorbing ethyl iodide multilayers.

4. Discussion

Multilayer CD_3I desorbs from clean Pd(1 1 1) at 127 K with the monolayer desorbing at 229 K (Figs. 1 and 2). The infrared spectrum of 8.0 L of CH_3I at 80 K on Pd(1 1 1) (Fig. 6) exhibits a series of features at 884, 1243 and 1428 cm^{-1}, which disappear as the surface is heated to 120 K. This temperature corresponds to both the multilayer desorption temperature (Fig. 1) as well as that at which the C–I bond starts to cleave [12,14]. This therefore indicates that these features are due to molecular methyl iodide on the surface. These peaks can be straightforwardly assigned by comparison with gas-phase methyl iodide [24] and the assignments are displayed in Table 1. Note, however, that the relative intensities of the multilayer 1243- and 884-cm^{-1} features vary with exposure. If the C–I bond of multilayer methyl iodide were oriented perpendicularly to the surface, according to the RAIRS surface selection rules, only modes of a_1 symmetry should be allowed if the molecule maintains its C_{3v} symmetry on the surface. This would result in only the 1243- and 2953-cm^{-1} modes being detected. Conversely, if the C–I axis were parallel to the surface, only e modes would be detected. Clearly, the detection of modes of both a_1 and e symmetry for the multilayer indicates that the C–I axis is oriented at some intermediate angle to the surface. In addition, it is clear that the intensity ratio of the 1243- (a_1) and 884-cm^{-1} (e) mode varies with exposure. The ratio

I(1243)/I(884) is tabulated as a function of methyl iodide exposure in Table 3. Since the 1243-cm^{-1} mode is of a_1 symmetry and that at 883 cm^{-1} of e symmetry, according to the above argument, this ratio should be infinity if the C–I bond is perpendicular to the surface, and zero if it is parallel. Clearly, the variation in this ratio as the exposure increases indicates that the methyl iodide orientation, while tilted throughout the whole measured exposure range, changes as the coverage increases.

Heating the surface to 120 K gives rise to broad features at 2932 and 1215 cm^{-1} with sharper peaks at 1411 and 884 cm^{-1}. As noted above, 120 K is close to both the multilayer desorption temperature and that at which substantial C–I bond cleavage is underway [12,14] and these features are assigned to the presence of a mixture of adsorbed methyl iodide [11] and methyl species. Again, these peaks can be assigned by comparison to gas-phase methyl iodide and the assignments are shown in Table 4. Since peaks of both a_1 and e symmetry are evident in the spectrum, this indicates that, after annealing to 120 K, the symmetry axis of the adsorbed species is tilted with respect to the surface. As the sample is heated to 200 and 220 K, the 884-cm^{-1} peak disappears and the spectrum consists of features at 1225 and 2932 cm^{-1}. These can again be assigned by comparison with the gas-phase spectrum and the assignments are also displayed in Table 4. Now only features of a_1 symmetry are seen indicating that the symmetry axis of the methyl group is oriented perpendicularly to the surface. Comparison with the methane desorption spectra for high methyl iodide coverages (Figs. 1 and 2) suggests that the low-temperature (191-K) state is associated with the broad feature centered at ~1215 cm^{-1}, while the high-temperature methane formation state is due to the hydrogenation of a methyl group with the C–Pd bond perpendicular to the surface. Heating to 170 K forms perpendicular methyl species and causes a significant decrease in intensity of the 1215-cm^{-1} feature (Fig. 6). C–I bond cleavage is complete at this temperature [12,14] so that the broad shoulder at 1215 cm^{-1} in this spectrum is entirely due to methyl species and the relatively large 884-cm^{-1} intensity implies that this is tilted on the surface indicating that the low-temperature (191-K) formation of methane is due to the hydrogenation of tilted methyl species, while the high-temperature state arises from the hydrogenation of perpendicular ones.

Table 3
Ratio of the intensity of the 1243-cm^{-1} mode to that of the 883-cm^{-1} peak as a function of methyl iodide exposure

CH_3I exposure/L	I(1243)/I(884)
1.0	0.6
2.0	1.8
8.0	1.4

Table 4
Assignments of the features in the RAIRS spectrum of methyl species (C_{3v} symmetry) formed by adsorbing methyl iodide on Pd(1 1 1) at 80 K and heating to 120 and 220 K (Fig. 6)

Symmetry	Mode	Gas-phase CH_3I/cm^{-1} [24]	CH_3I/Pd(1 1 1)/cm^{-1} (120 K)	CH_3I/Pd(1 1 1)/cm^{-1} (220 K)
$e(x,y)$	$\nu_a(CH_3)$	3060	–	–
$a_1(z)$	$\nu_s(CH_3)$	2933	2932	2932
$e(x,y)$	$\delta_a(CH_3)$	1436	–	–
$a_1(z)$	$\delta_s(CH_3)$	1252	1215	1225
$e(x,y)$	$\rho(CH_3)$	882	884	–

δ—deformation, ρ—rock, ν—stretch.

It is also clear, however, from the TPD data of Figs. 2 and 3 that the coverage has a profound effect on the hydrogenation kinetics. Comparing these spectra reveals that hydrogen desorbs at ~359 K while, at low coverages, methane is evolved in a single peak at ~219 K. As the exposure increases to 2 L, the 219 K (methane) peak grows, while the 359 K (deuterium) feature decreases slightly in intensity. Since the 219-K desorption state appears to shift smoothly toward the 191-K state as the methyl iodide coverage increases, this implies that the 219-K state is similarly due to the hydrogenation of a tilted methyl species. The decrease in the amount of hydrogen formed as the coverage increases is then ascribed to the lack of space available on the surface for dehydrogenation. This suggestion is supported by the further decrease in the amount of hydrogen desorption that occurs as the exposure is increased to saturation (6 L). Thus, the relative rates of hydrogenation and dehydrogenation appear to depend on the neighboring sites available to accept the hydrogen and is limited by the crowded surface. As the exposure increases to 3 L, another state appears at ∼270 K, which shifts to 304 K as the coverage approaches saturation. The exposure of 3 L corresponds to ∼50% of the saturation coverage and the high-temperature methane state was suggested above to be due to the hydrogenation of a perpendicular methyl species. In this case, presumably there is insufficient hydrogen on the surface to completely consume the more easily hydrogenated, tilted methyl state so that it converts into a more stable, but less easily hydrogenated perpendicular state. This conjecture is confirmed by the desorption spectrum in Fig. 4 which shows the effect of pre-dosing the surface with deuterium (10 L) and then saturating with methyl iodide. Now there is sufficient hydrogen on the surface to completely react with the tilted methyl species on the surface which desorbs in a state at ∼209 K.

The variation in the temperature of the methane desorption state when the CD_3I exposure is increased (Fig. 5) is interesting. The intensity of this feature increases with increasing CD_3I exposure as expected. However, surprisingly the peak temperature increases with increasing CD_3I exposure, while it would be anticipated that increasing the methyl iodide (and correspondingly the methyl) coverage would result in a decrease in desorption temperature. The observation that the desorption temperature increases with increasing exposure suggests that there are strong interactions between the adsorbed species that affects the activation energy to methane formation.

It has been suggested that methyl species adsorbed on Pd(1 1 1), when formed from methanol, can be stable up to ∼400 K [28]. The detection of methane desorption states at ∼304 K (Fig. 1) confirms that the methyl species with the C_3 symmetry axis oriented perpendicular to the surface is stable to at least this temperature. However, in addition, a small 4-amu feature is detected centered at ∼360 K with a tail extending to a little above 400 K. The data of Fig. 4, for example, shows that atomic deuterium on the surface desorbs at ∼300 K, indicating that the high-temperature 4-amu state in Fig. 1 is due to the thermal decomposition of a surface CH_x species. It is not clear however, whether this is some remaining perpendicular methyl species or a methylene species deriving from this. To explore this possibility, methylene species were grafted onto the surface by reacting it with CH_2I_2. The resulting RAIRS spectra are displayed in Fig. 7. Comparing the spectra obtained for methylene species (Fig. 7) with the RAIRS data obtained by warming a CH_3-covered surface (Fig. 6), it is found that the formation of CH_2 species at high temperatures is not a major reaction pathway.

Assuming that the methane formation rate from methyl iodide on metal surfaces is limited by the rate of α-hydrogen elimination to yield the available hydrogen allows the rate on Pd(1 1 1) to be compared with those for other transition metals. Methane is formed at 219 K from methyl iodide at low coverages on Pd(1 1 1) (Fig. 2), close to the temperature of 215 K found on Pd(1 0 0) [9]. Note, however, that these values must be used with caution since methane desorbs at only slightly lower temperatures (∼190 K, Fig. 5) from low cov erages of methyl iodide from hydrogen-covered Pd(1 1 1). However, the differences are sufficiently large that the methane formation temperature of 219 K for low coverages on methyl iodide on Pd(1 1 1) likely reflects the rate of hydrogen formation. The corresponding temperatures are 170 K on Ru(0 0 1) [29], 230 K on Ni(1 0 0) [10] and 260 K on Pt(1 1 1) [11] showing the expected trend of decreasing temperature, indicating increased dehydrogenation activity, on moving toward the left of the d-transition series. A similar comparison for β-hydrogen elimination, measured from the ethylene desorption temperature from adsorbed ethyl species, which occurs at 175 K on Pd(1 1 1) (Fig. 8) shows that this is close to the value on Pd(1 0 0) of 180 K [30]. Comparing with the ethylene desorption temperatures from ethyl species on Ni(1 0 0) (160 K [31]), Pt(1 1 1) (180 K [32]), Rh(1 1 1) (210 K [33]), Fe(1 0 0) (220 K [34]), Cu(1 0 0) (250 K [35]) and Au(1 1 1) (265 K [36]), shows that the trend in reactivity in this case is that this increases in going upwards and to the left in the periodic table. Finally, the rate of β-hydride elimination, which has an activation energy of ∼10.5 kcal/mol on Pd(1 1 1), is more rapid than the rate of α-hydride elimination which has an activation energy of ~13.0 kcal/mol.

5. Conclusions

Methyl iodide adsorbs on Pd(1 1 1) at 80 K to form a molecular overlayer with subsequent adsorption into a multilayer where the methyl iodide orientation changes with coverage. The multilayer desorbs at ~130 K and unreacted methyl iodide desorbs from the surface at ~229 K. Self-hydrogenation of methyl iodide is found in two states at high coverages where the low-temperature (~191-K) state is proposed to be due to the hydrogenation of tilted methyl species while the high-temperature (304-K) state is due to the hydrogenation of perpendicular methyl species. A single methane desorption state is found at lower coverages at ~219 K. Pre-dosing the surface with hydrogen completely suppresses the high-temperature methane desorption state yielding a peak between ~189 and 207 K depending on methyl iodide exposure. The rates of α- and β-hydride elimination on Pd(1 1 1) are in accord with trends found previously on the noble metals where the rate of β-hydride elimination is faster than the rate of α-hydride elimination.

Acknowledgements

We gratefully acknowledge support of this work by the US Department of Energy, Division of Chemical Sciences, Office of Basic Energy Sciences, under grant no. DE-FG02-92ER14289.

References

[1] F. Zaera, Chem. Rev. 95 (1995) 2651.
[2] B.E. Bent, Chem. Rev. 96 (1996) 1361.
[3] G. Wu, B. Bartlett, W.T. Tysoe, Langmuir 14 (1998) 1435.
[4] D. Stacchiola, S. Azad, L. Burkholder, W.T. Tysoe, J. Phys. Chem. B 105 (2001) 11233.
[5] X.-L. Zhou, F. Solymosi, P.M. Blass, K.C. Cannon, J.M. White, Surf. Sci. 219 (1989) 294.
[6] M.X. Zhang, S.K. To, A. Paul, L. Avila, B.E. Bent, K. Nishikida, Surf. Sci. 325 (1995) 102.
[7] X.-L. Zhou, J.M. White, J. Phys. Chem. 95 (1991) 5575.
[8] G. Wu, D. Stacchiola, M. Kaltchev, W.T. Tysoe, J. Am. Chem. Soc. 122 (2000) 8232.
[9] F. Solymosi, K. Revész, J. Am. Chem. Soc. 113 (1991) 9145.
[10] S. Tjandra, F. Zaera, Langmuir 8 (1992) 2090.
[11] F. Zaera, H.J. Hoffmann, J. Phys. Chem. 95 (1991) 6297.
[12] J.J. Chen, N. Winograd, Surf. Sci. 314 (1994) 188.
[13] D. Stacchiola, L. Burkholder, W.T. Tysoe, Surf. Sci. 511 (2002) 215.
[14] M.T. Buelow, B. Immaraporn, A.J. Gellman, J. Catal. 203 (2001) 41.
[15] C.W.J. Bol, C.M. Friend, J. Am. Chem. Soc. 117 (1995) 11572.
[16] I. Kovács, F. Solymosi, J. Mol. Catal. A 141 (1999) 31.
[17] F. Solymosi, I. Kovács, K. Revész, Surf. Sci. 356 (1996) 121.
[18] A. Kis, J. Kis, F. Solymosi, Surf. Sci. 459 (2000) 149.
[19] H. Wu, H. Hsu, C. Chiang, J. Am. Chem. Soc. 121 (1999) 4433.
[20] F. Solymosi, I. Kovács, Surf. Sci. 296 (1993) 171.
[21] S. Monin, P.H. McBreen, Surf. Sci. 264 (1992) 341.
[22] G. Wu, M. Kaltchev, W.T. Tysoe, Surf. Rev. Lett. 6 (1999) 13.
[23] M. Kaltchev, W.T. Tysoe, J. Catal. 196 (2000) 40.
[24] T. Shimanouchi, Molecular vibrational frequencies, in: W.G. Mallard, P.J. Linstrom (Eds.), NIST Chemistry WebBook, NIST Standard Reference Database Number 69, November 1998, National Institute of Standards and Technology, Gaithersburg MD, 20899.
[25] J.N. Kendo, T. Higashi, H. Yamamoto, M. Hara, K. Domem, T. Onishi, Surf. Sci. 349 (1996) 294.
[26] G. Wu, M. Kaltchev, W.T. Tysoe, Surf. Rev. Lett. 6 (1999) 13.
[27] G. Wu, D. Stacchiola, M. Collins, W.T. Tysoe, Surf. Rev. Lett. 3/4 (2001) 303.
[28] R.J. Lewis, Z.C. Jiang, N. Winograd, J. Am. Chem. Soc. 110 (1988) 4431.
[29] Y. Zhou, M.A. Henderson, W.M. Feng, J.M. White, Surf. Sci. 224 (1989) 386.
[30] T. Kovács, F. Solymosi, J. Phys. Chem. 97 (1993) 11056.
[31] S. Tjandra, F. Zaera, J. Vac. Sci. Technol. A 10 (1992) 404.
[32] F. Zaera, J. Phys. Chem. 94 (1990) 8350.
[33] F. Solymosi, L. Bugyi, A. Oszkó, Langmuir 12 (1996) 4145.
[34] M.L. Burke, R.J. Madix, J. Am. Chem. Soc. 113 (1991) 2675.
[35] C.J. Jenks, M. Xi, M.X. Yang, B.E. Bent, J. Phys. Chem. 98 (1994) 2152.
[36] A. Paul, M.X. Yang, B.E. Bent, Surf. Sci. 297 (1993) 327.